Dynamics of the Flexible Loop of Triosephosphate Isomerase: The Loop Motion Is Not Ligand Gated†

John C. Williams and Ann E. McDermott*

Department of Chemistry, Columbia University, New York, New York 10027

Received July 29, 1994; Revised Manuscript Received December 22, 1994®

ABSTRACT: Using solid-state deuterium NMR, we have measured the motion of the flexible loop of triosephosphate isomerase (TIM) with and without substrate and transition-state analogs. The measurements were carried out on a catalytically competent mutant of TIM W90Y W157F containing a single tryptophan (W168) in the flexible loop; W168 is the only strictly conserved tryptophan in the currently available TIM sequences. The solid-state NMR samples were prepared by precipitation using polyethylene glycol, and kinetic analysis of the PEG-precipitated TIM gave values for k_{cat}, K_m, and K_I similar to those measured in solution for the substrate and substrate and transition-state analogs. Deuterium NMR spectra of samples prepared with tryptophan labeled at the indole positions with and without any substrate or analogs indicate that the loop jumps between two conformations at a rate of 3×10^4 s^{-1} (from the predominant to the less populated form) with a population ratio of 10:1. Surprisingly, spectra of TIM ligated with a substrate analog, glycerol 3-phosphate (G3P), or with a tight-binding transition-state analog, phosphoglycolate (PGA), show that the loop moves with a rate similar to the rate in the empty enzyme and also has a similar population ratio for the two conformers. *This observation indicates that loop closure is not ligand gated but is a natural motion of the protein. Furthermore, the measured rate is approximately matched to the turnover time.* We did not observe a signal for TIM labeled with α-deuteriotryptophan, although it was prepared in a fashion analogous to the ring-labeled sample and had a specific activity and protein concentration comparable to the latter. For this deuterium concentration, we would expect to observe the NMR signal unless the deuterium relaxation were very slow. The hypothesis that the spin−lattice relaxation of the α-deuteron is very slow would be consistent with the observed dynamics of the ring-deuterated TIM.

Many loops which connect two regions of secondary structure in enzymes coined Ω loops (Leszczynski & Rose, 1986) exhibit two distinct structures depending on the presence or absence of a substrate analog compound. The loop partly envelops the substrate in the so-called closed state, completing the active site and excluding solvent (Branden & Tooze, 1991; Chothia et al., 1989; Kempner, 1993). In the absence of substrate (the open state), these loops often display large Debye−Waller factors, or they are invisible altogether because of their mobility. The substrate can bind and product can escape when the loop is in the open state; when the loop is in the closed state these processes are impossible for steric reasons. These observations suggest that the conformational changes in loops are needed for enzymatic catalysis. Such conformational changes provide a concrete example of an induced fit of an enzyme to a ligand. The importance of the conformational change in these loops is well appreciated; however, very little is known about their dynamics and particularly the time scale associated with these dynamics. With this in mind, we have chosen to apply solid-state NMR[1] to study the flexible loop in triosephosphate isomerase (TIM).

TIM is one of the first proteins for which large conformational changes in a loop region were demonstrated. It catalyzes the interconversion of dihydroxyacetone 3-phosphate (DHAP) and glyceraldehyde 3-phosphate (GAP), which consists of a series of simple proton-transfer reactions (Rose, 1962). This interconversion does not require any cofactors and is reversible with an overall driving force of 1.8 kcal/mol. Detailed kinetic experiments involving isotopically labeled substrate and product have provided evidence for the catalytic landscape and indicate that diffusion and product release are rate limiting (Knowles & Albery, 1977, and references therein). Studies employing viscogenic agents demonstrate that the enzyme-catalyzed conversion is sensitive to viscosity in a fashion consistent with a diffusion-controlled process, implying that the highest barriers are associated with substrate binding and product release (Blacklow et al., 1988; Knowles & Albery, 1977).

Crystallographic studies have shown that TIM is an αβ-barrel with one loop region of ten amino acids above the

† Acknowledgment is made to the Donors of the Petroleum Research Fund, administered by the American Chemical Society, for partial support of this research. A.E.M. acknowledges support from Kanagawa Academy of Science and Technology. J.C.W. acknowledges support from NIH Biophysics Training Grant GM98281.

® Abstract published in *Advance ACS Abstracts,* February 15, 1995.

[1] Abbreviations: DANTE, NMR pulse sequence for selective inversion; DHAP, dihydroxyacetone 3-phosphate; FID, free induction decay; GAP, glyceraldehyde 3-phosphate; G3P, glycerol 3-phosphate; IPTG, isopropyl β-D-thiogalactopyranoside; NMR, nuclear magnetic resonance; PEG, polyethlene glycol (average molecular weight 3400); PDB, Protein Data Bank; PGA, phosphoglycolic acid; PGH, phosphohydroxamate; RMS, root mean square (deviations); SDS−PAGE, sodium dodecyl sulfate−polyacrylamide gel electrophoresis; T_1, spin−lattice relaxation time; TIM, triosephosphate isomerase.

0006-2960/95/0434-8309$09.00/0

active site, loop 6 (residues 166−178), which exhibits two structures depending on the binding of substrate and transition-state analogs (Figure 1) (Alber et al., 1981; Davenport et al., 1991; Lolis et al., 1990; Lolis & Petsko, , 1990; Noble et al., 1991; Verlinde et al., 1991; Wierenga et al., 1991a,b, 1992). This conformational change excludes bulk solvent from the active site and may modify the dielectric at the active site (Lolis & Petsko, 1990). These high-resolution structures show that the amide NH group of glycine 171 in the loop makes a hydrogen bond to the phosphate group of substrate and transition-state analogs. Deletion of four amino acids in the loop region caused a substantial increase in the production of methylglyoxal and inorganic phosphate (Pompliano et al., 1990). This observation suggests that the hydrogen bond from the loop holds the phosphate out of the enediol plane, thus reducing orbital overlap and preventing phosphate elimination. Recent solid-state NMR methods using the tight-binding transition-state analog, phosphoglycolate (PGA), directly confirmed the out-of-plane conformation (Tomita et al., 1994).

Structural data have provided much insight into the mechanism of the conformational transition of the loop. Detailed analysis of the atomic coordinates generated from the crystal structures shows that the loop moves as much as 8 Å between the open and closed conformations. Analysis of the flexible loop region indicates that the loop acts like a rigid lid. Two regions on either side of the loop act as hinges and consist of two amino acids on one side and three on the other. The dihedral angles of the amino acids in the hinged regions are anticorrelated, which should afford a low steric transition barrier between the open and closed states (Joseph et al., 1990). Interestingly, another large change in the transition between the two states corresponds to a large change in the Ramanchandran ϕ,ψ dihedral angles of the strictly conserved serine 211 which resides in the adjacent loop, loop 7 (S213 in trypanosomal TIM) (Noble et al., 1991).

One approach for addressing dynamics of macromolecules is computational methods. Molecular dynamics simulations of the open structure of TIM show that the loop closes or opens in a jumplike fashion within approximately 20 ps at 2000 K. Another simulation with a TSA bound showed that when the loop started in the closed position, it remained closed throughout the simulation (Joseph et al., 1990). Additional molecular mechanics studies predict that the loop only closes in the presence of substrate analogs (Brown & Kollman, 1987) while, in the absence of substrate, the loop jumps between the two conformers with equal populations and a correlation time of 0.5 ns (Wade et al., 1993).

For TIM and other enzymes there is typically very little experimental information concerning large amplitude motions that occur on the time scale of ligand binding and catalytic turnover. Two common methods for characterizing protein motions are optical methods and NMR. Relaxation (T_1) measurements by solution NMR detect protein dynamics by probing spectral densities which occur at several frequencies, and these methods are applicable to proteins smaller than ~30 kDa. The relaxation times are often interpreted in terms of the model-free formalism (Lipari & Szabo, 1982) which utilizes an isotropic overall correlation time, a correlation time for internal degrees of freedom, and a parameter related to the amplitude for these internal modes, which is referred to as a generalized order parameter. Information garnered in these measurements best reflects contributions from motions in the range of 10^8-10^{12} s^{-1} but motions in the kilohertz regime are sometimes implicated as well (Peng & Wagner, 1992). Chemical-exchange NMR methods characterize slower dynamics. These methods utilize two well-resolved lines corresponding to the different conformations. Recently, this method has been successfully applied to dihydrofolate reductase (Falzone et al., 1994). Optical methods either measure very fast dynamics (10^9-10^{15} s^{-1}), or, with stop-flow or heat or pressure-jump techniques, measure very slow dynamics (10^4-10^{-3} s^{-1}) (Hart et al., 1993; Waldman et al., 1988). The relatively poor ability of these methods to probe motions that occur in the microsecond regime places an impediment for studying certain motions, particularly those associated with rapid catalytic turnover rates.

Solid-state deuterium NMR, on the other hand, is capable of providing detailed information continuously over many orders of magnitude in time ($10^{-1}-10^{10}$ s^{-1}). Three different solid-state NMR experiments are used to cover this range of time scales, each taking advantage of the orientationally dependent quadrupolar powder pattern. The τ-dependent line-shape experiment covers motions of the order 10^3-10^8 s^{-1}. Motions on this time scale can result in a loss of spectral intensity and a characteristically distorted line shape (Beshah et al., 1987; Rice et al., 1981). The second experiment, T_1 anisotropy, follows the relaxation of the quadrupole line shape after a broad-band inversion pulse. The rate of relaxation is orientation dependent, causing different parts of the spectra to relax at different rates (Beshah et al., 1987; Griffin, 1981; Hiyama et al., 1986). Motions with a characteristic rate of 10^7-10^{12} s^{-1} that modulate the C−D bond vector with respect to the applied static field drive these relaxation processes. The relaxation rate is determined by the rate of motion, populations of the states, and angles between the corresponding bond vectors, while the anisotropy is large if the populations are nearly equal and the angles are large. Finally, a family of experiments are capable of measuring motions on slower time scale, with a lower limit set by the spin−lattice relaxation time, ~$0.1-10$ s^{-1} (Spiess, 1980; Vold & Vold, 1991; Williams & McDermott, 1993). Spectra can be simulated explicitly for each of these methods, given a model of the motion. These simulations provide information about the populations of different conformers, the rate of the motion connecting these conformers, and angular excursions between each conformer. Moreover, this technique does not require initiation of the reaction and does not have a molecular weight cutoff. The method, however, does require the specific labeling of one residue at the position of interest. Previous studies of biomolecules employing solid-state deuterium NMR have characterized methyl group hops (Copié et al., 1994; Keniry et al., 1984; Kinsey et al., 1981), phenyl ring flips (Rice et al., 1981), and backbone fluctuations (Usha et al., 1991). This report describes deuterium SSNMR measurements of the dynamics of a single tryptophan (W168) in the flexible loop of the mutant W90Y W157F of yeast TIM. The line-shape measurements with quadrupolar echo pulse sequences emphasize the time scale of enzymatic turnover. We utilized ligands that mimic the substrate and the transition state of the reaction to investigate the dependence of the loop motion on the arrival of the ligand and the progress of the reaction. These compounds and the corresponding proposed reactive intermediates are drawn in Figure 2.

EXPERIMENTAL PROCEDURES

All reagents used were purchased from Aldrich or Sigma with the exception of GDH and NADH, which were purchased from Boehringer Mannheim.

Preparation of Labeled Tryptophan. (A) Indole Ring Labeled Deuteriotryptophan. Tryptophan deuterated at all of the five positions of the indole ring was prepared according to Matthews et al. (1977). Solution NMR of the deuterated tryptophan showed 95% incorporation at all positions of the indole ring.

(B) α-Labeled Deuteriotryptophan. Tryptophan deuterated at the α-position was carried out enzymatically using serine and indole as precursors and a strain of *Escherichia coli* rich in tryptophan synthetase (generous gift from Prof. Charles Yanofsky, Biology Deptartment, Stanford University) (Drewe & Dunn, 1985; Schneider et al., 1981). The cells containing the overexpression system for tryptophan synthetase were grown, harvested, and lyophilized. The cells were then resuspended in a deuterated 100 mM phosphate−100 mM KCl buffer (pH = 7.0) in order to exchange labile protons. The exchanged cells were collected by centrifugation and lyophilized a second time. The labile protons of serine were simply exchanged in a solution of D_2O, and the solvent was removed by rotary evaporation. Exchanged serine (2 g), indole (3 g), pyridoxal 5-phosphate (100 mg), and exchanged cells (250 mg) were added to 10 mL of a freshly prepared deuterated phosphate−KCl buffer. The solution was tightly sealed and placed in an incubator set at 37 °C for 2 days.

The reaction was quenched with 1 M HCl, and the pH was adjusted to 2.2. The cells were removed by centrifugation, and the supernatant containing the tryptophan was passed over a column of Dowex-50 (van der Berg et al., 1989). The column was washed with 3 volumes of phosphate buffer at a pH of 2.4. The tryptophan was then eluted with 1 M NH_4OH. Fractions containing tryptophan were pooled, and the solvent was removed by rotary evaporation. The tryptophan was recrystallized twice from an ethanol−water solution. The yield was >90%, and incorporation was greater than 99% as measured by solution NMR.

Preparation of Labeled Protein. The plasmid containing the mutant TIM (generous gift of Professor Sampson of SUNY, Stonybrook, and Professor Knowles of Harvard University) was transformed into a competent tryptophan auxotroph of *E. coli* (generous gift from Dr. Goodin) using the method outlined by Chung et al., (1989). Growth conditions yielding maximum protein expression were explored. The best conditions required initial growth in LB broth supplemented with 50 μg/mL ampicillin at 37 °C and good aeration. When the cell density reached an optical density at 600 nm of 0.3, the cells were gently centrifuged and resuspended in a defined medium[2] supplemented with 250 mg/L ring-deuterated tryptophan, 50 mg/L ampicillin, and 0.4 mM IPTG. After approximately 20 h the cells were harvested by centrifugation, and the cell pellets were resuspended in approximately 20 mL of buffer A.[2] The resuspended cells were passed through a French press (Aminco) once, and the cellular debris was removed by centrifugation at 10000*g* for 20 min. (All purification steps hereafter were performed at room temperature.) Ammonium sulfate was added to the supernatant, resulting in a 40% saturated solution. After 1 h at room temperature, precipitated material was removed again by centrifugation at 10000*g* for 20 min. Ammonium sulfate was then added to the supernatant to bring it to 75% saturation, and again the solution was allowed to equilibrate for 1 h. Centrifugation of the resulting solution produced off-white pellets containing the labeled TIM. These pellets were then resuspended in a minimal amount of buffer B[2] and extensively dialyzed against the same buffer. The dialyzed protein solution was then titrated with a freshly prepared solution of protamine sulfate (25 mg/mL) to remove DNA; typically 2.5−25 μL of the protamine sulfate solution was added to 50 μL of the protein solution. After 1 h, the titrated samples were centrifuged, and the ratio of absorbance at 260 nm to that at 280 nm and the enzymatic activity were measured. (Excess protamine sulfate caused protein precipitation later in the preparation as measured by activity.) With most of the DNA removed, the pale yellow protein solution was dialyzed exhaustively against buffer C[2] and then passed over a Sepharose Q column equilibrated against the same buffer to remove a yellow contaminant. An enzymatic assay of the protein at this point generally shows a 2-fold increase in total activity as compared to crude protein extract. Finally, the protein was dialyzed against buffer D[2] and bound onto a Sepharose Q column preequilibrated with the same buffer. The protein was then eluted using buffer D with a gradient of KCl up to 150 mM and collected by fractionation. SDS−PAGE showed a small contaminant at approximately 70 kDa, which could be partially purified by a second gradient as described above. The fractions containing the labeled TIM were then pooled and precipitated using ammonium sulfate.

Kinetics of TIM in PEG. The measurement of the kinetics of TIM in the presence and absence of PEG was carried out using the standard GDH-linked assay (Albery & Knowles, 1976). The assay mixture included GDH in large excess, NADH, and GAP in buffer A.[2] The absorbance at 340 nm was then monitored at intervals of 6 s over 2 min. Once the baseline was established, 0.25 unit of TIM was placed in the cuvette, which was vigorously shaken and replaced in the spectrometer. The decrease in absorbance at 340 nm was linear in time and proportional to V_{max}, since a saturating substrate concentration was used. Substrate concentration was then varied, and these data were analyzed using a Lineweaver−Burk relationship giving values for k_{cat} and K_m as indicated in Table 1. Similar measurements were carried out in 30% PEG (w/v).

When the TIM in 30% PEG was centrifuged at 13500*g* for 10 min and at concentrations typically used for assays (10−100 ng/mL), approximately 90% formed a pellet in an active form. Thus the activity assays performed in 30% PEG

[2] Media used in TIM preparation and characterization: LB, Luria−Bertani broth; defined media (list provided by Dr. Dave Goodin, Scripps Research Institute), 120 mL of 10× concentrated M9 salts, 940 mL of a solution containing 1 g/L Ala, Pro, Tyr, Ile, Phe, Lys, Asp, Val, Ser, Thr, Glu, and Arg, 120 mL of a solution containing 10 g/L His, Leu, and Met, 2.5 mL of a 50% (v/v) solution of glycerol, 1.2 mL of a 100 mM solution of $CuCl_2$, 1.2 mL of a 1 M solution of $MgSO_4$, and 12 mL of a 0.1% solution of thiamin; buffer A, 50 mM Tris, 50 mM NaCl, 1 mM EDTA, 1 mM DTT, and 100 mM PMSF, pH = 7.8; buffer B, 50 mM Tris, 300 mM NaCl, 1 mM EDTA, 1 mM DTT, and 100 mM PMSF, pH = 7.8; buffer C, 20 mM Tris, 100 mM NaCl, and 100 mM PMSF, pH = 7.8; buffer D, 10 mM Tris, pH = 7.8; TIM assay conditions, buffer A used with 0.3 mM NADH, 25 μg/mL freshly prepared GDH (glyceraldehyde dehydrogenase, Boehringer Mannheim), and saturating concentrations of GAP (ca. 3 mM).

and reported in Table 1 are assumed to reflect primarily precipitated TIM. The K_I values for PGA and G3P were measured in the same fashion varying substrate and inhibitor concentrations independently.

NMR Samples. (A) Empty Sample. The ammonium sulfate precipitated TIM was resuspended in buffer A and exhaustively dialyzed against the same buffer. The protein solution was then precipitated with PEG 3400 (30% w/v). After approximately 1 h, the milky white solution was pelleted by centrifugation and resuspended in buffer A prepared from deuterium-depleted water. The sample was allowed to exchange overnight before precipitation by PEG. The milky white solution was then pelleted by centrifugation at 13400*g* for 8 h. The supernatant was removed, and the pellet was placed in a sample holder. Activity assays of the protein solution before the final precipitation and of the supernatant after precipitation indicated that most samples contained approximately 20−50 mg. Assays after the NMR experiments indicated undetectable loss of specific activity, although total protein was often less because of poor recovery.

(B) G3P and PGA Samples. The samples with substrate and transition-state analogs were prepared in a fashion similar to that of the empty sample; however, the analogs were added before the last precipitation. We based our procedures for binding ligands to precipitated TIM on those used successfully by crystallographers to both soak and cocrystallize TIM with these ligands (Davenport et al., 1991; Lolis & Petsko, 1990; Alber et al., 1981). Evidence for the binding of TSA compounds to TIM microprecipitates has been obtained in a variety of ways. The simplest assay is the inhibition of dilute TIM in 30% PEG, discussed above. The dilute TIM in 30% PEG is insoluble and yet is active, as discussed above, and according to kinetic measurements under these conditions TIM binds these inhibitors competitively. In a separate study we have measured the CPMAS spectrum of doubly ^{13}C-labeled PGA bound to TIM microcrystals (Tomita et al., 1994) prepared in the same way as our deuterated samples were. The simple fact that a sharp ^{13}C signal resulted from CPMAS proves clearly that the inhibitor is bound to a well-defined solid-state environment. In these deuterium SSNMR experiments we observed a statistically significant effect of the ligands on the deuterium relaxation time, T_1 *(vide infra).* Finally, centrifugation of a stoichiometric equivalence of PGA to TIM active sites in a microcrystalline suspension resulted in the disappearence of PGA in the supernatant as measured by ^{31}P solution NMR.

The typical volume of precipitated protein samples was approximately 200 μL. The volume before precipitation was typically 1 mL. The amount of analog added to the suspended protein solution was greater than 50 times that of the number of active sites and always well above the K_I.

NMR Experiments. All spectra were taken on a Chemagnetics CMX-400 with the Chemagnetics wide-line probe and variable temperature apparatus. The pulse lengths were typically 1.9−2.2 μs, and a spectral width of 2 MHz was utilized.

τ-dependent spectra were collected using the standard eight-phase quadrupolar echo pulse sequence. T_1 values were in the range of 200 ms, and recycle delays of 1 s were used. The data length was set to 256 points; the data were baseline corrected and zero filled to 2048 points. Line broadening of 2 kHz was applied to each FID before Fourier transformation.

The pulse lengths for the DANTE pulse train were 200 ns and pulse spacing of 12.96 μs. The number of pulses in the train was varied to optimize the inversion efficiency. Typically the train consisted of 23 pulses. The frequency used for the selective inversion on the TIM samples was ±63 kHz. Recovery times of 10 μs, 100 μs, 1 ms, 10 ms, and 100 ms were used. A second set of data interleaved between each recovery time was collected without the DANTE inversion and used for difference spectra. The data were processed in the same manner as the τ-dependent spectra.

Simulations. Simulations of the τ-dependent spectra were carried out using the Turbopowder program (Speyer et al., 1989; Wittebort et al., 1987). This program presupposes a specific motional model and requires a set of rates, sites (defined by a set of Euler angles), and a population at each site. For example, a deuteron on phenylalanine undergoes a ring flip which is modeled as a two-site jump with equal populations at each site. The rate is then varied to reproduce the experimental line shape. Our choice of a two-site model with unequal populations is justified by the crystal structures of TIM with and without analogs and by the molecular dynamics studies. However, it is not the only model that is consistent with the NMR data. The populations, the angle, and the rate between the two sites were then individually varied, producing a family of fits.

In order to estimate an appropriate value for the angular excursions used in the simulated spectra, we superimposed each monomer of the three reported X-ray structures of yeast TIM (taken from the PDB) by minimizing the RMS deviation of the α carbons. The locations of all six indole rings were therefore known in a common coordinate frame. Euler angles for the excursion of each deuteron on the indole ring could then be calculated for the open and closed states or for any pair of monomers. These angles were used in the simulation shown in Figure 4.

RESULTS AND DISCUSSION

Solid-State Samples. In order to measure the loop dynamics, we obtained a mutant of TIM (W90Y W157F) which has only one tryptophan at its conserved position in the loop (W168) and displays normal Michaelis−Menten kinetics (Sampson & Knowles, 1992a,b). The positions of this tryptophan in the closed and open states are shown in Figure 1. Tumbling of the protein samples was arrested by precipitation with either ammonium sulfate or PEG, since whole-body rotation (such as would occur in solution) interferes with measurements of internal motions. Kinetic measurements were carried out in order to characterize the effect of precipitation on TIM. After addition of 5% (w/v) ammonium sulfate there was no detectable activity. Samples containing 30% (w/v) PEG exhibited nearly normal kinetics. The inhibition constants for the substrate and transition-state analogs used in the dynamics study and the Michaelis−Menten kinetic parameters were measured and are given in Table 1.

The protein suspension in PEG scatters light noticeably, and after centrifugation at 12000*g* for 15 min the enzymatic activity is associated with the pellet, demonstrating clearly that in the presence of PEG TIM forms microcrystals. The similarity in the turnover number and binding constants for the two samples indicates that the protein is not significantly

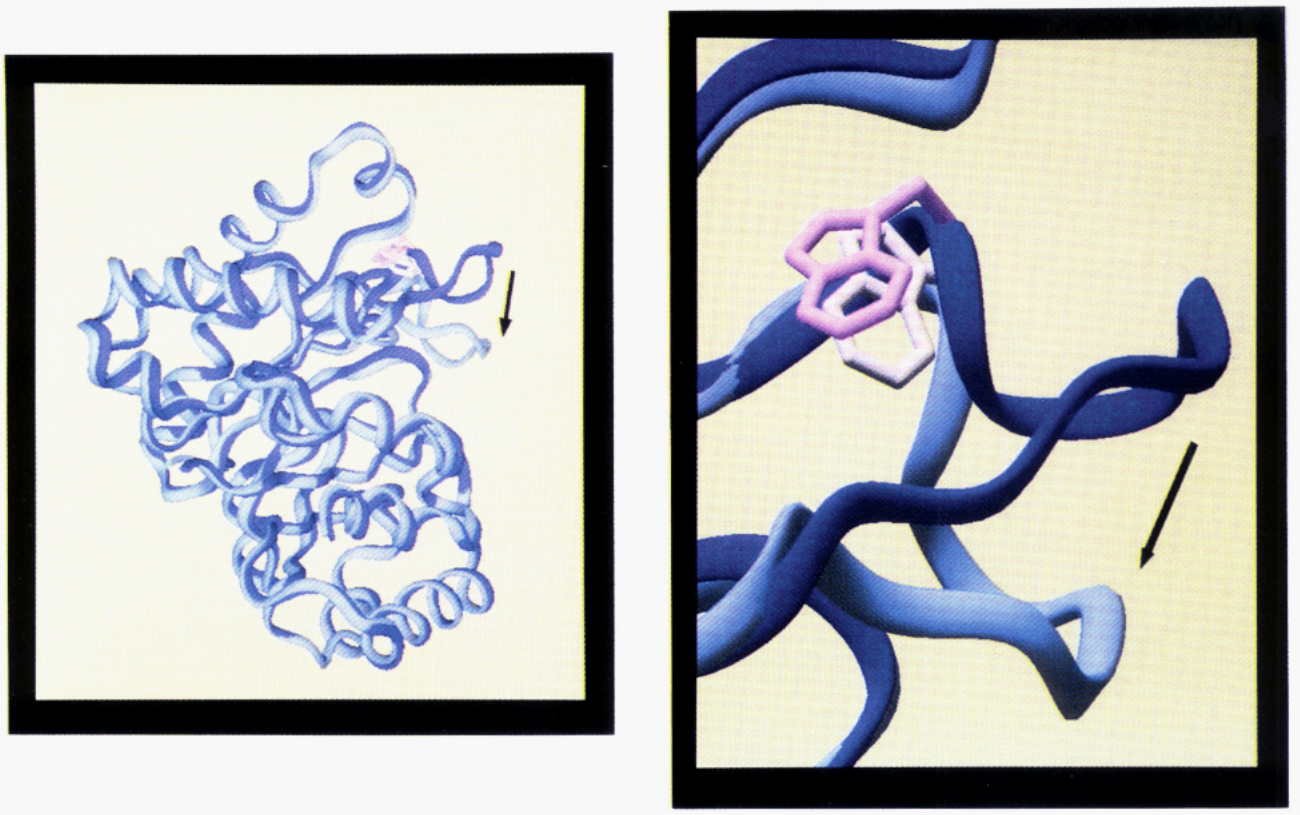

FIGURE 1: Two views of the opened and closed states of TIM, in which the purple is the closed state (yeast enzyme structure: 3YPI in the PDB) and the blue is the open state (PGH-ligated structure of the yeast enzyme: 1YPI), which have been superimposed by rotation and translation operations that minimized the RMS deviations in the positions of the α carbons of the backbone. Left panel: As has been previously noted, the major change between the two conformations resides mainly in loop 6 (Joseph et al., 1990; Wierenga et al., 1991a,b). Right panel: Close-up view of the flexible loop showing the position of the indole ring in the two states. Excursion angles for the ring deuterons are in the range 18−44°, depending on the particular deuteron, if the barrel is assumed to be static.

Table 1: Kinetic Data of TIM and Precipitated TIM[a]

	TIM	PEG−TIM
k_{cat} (s^{-1})	5500	3500
K_m for GAP (M)	1.5×10^{-4}	4.4×10^{-4}
K_I for PGA (M)	1.3×10^{-6}	4.3×10^{-6}
K_I for G3P (M)	4.4×10^{-4}	1.6×10^{-4}

[a] Errors in each measurement are less than 25% RSD.

altered by PEG precipitation. *We conclude from these kinetic assays that loop motions needed for activity do occur in the microcrystalline samples.*

Loop Dynamics. In order to characterize the dynamics of the flexible loop of TIM, we performed three different deuterium NMR experiments: τ-dependent quadrupolar echo experiments, T_1 anisotropy experiments, and DANTE inversion−recovery experiments. Loop motions were characterized in three samples representing three states along the reaction coordinate from GAP to DHAP (Figure 2).

Fast Dynamics and T_1 Anisotropy. T_1 inversion recovery experiments of the deuterium signal of ring-labeled TIM were done for four different preparations: an empty sample in PEG, a sample ligated with G3P and precipitated in PEG, a sample ligated with PGA and precipitated in PEG, and a sample precipitated in ammonium sulfate (Figure 3). The spectra showed weak anisotropy within the experimental signal-to-noise ratio, and consequently we only report a single T_1 value. The three samples exhibited T_1 values of 0.23 ± 0.05, 0.6 ± 0.2, 0.14 ± 0.05, and 0.28 ± 0.05 s for the empty TIM in PEG, the sample ligated with G3P, the sample ligated with PGA, and the sample precipitated in ammonium sulfate, respectively. The error range was mainly determined by the poor signal-to-noise ratio of the data and in the case of G3P the choice of delay times. Despite the large error in these measurements, they offer direct evidence for local motions in the tryptophan ring on the low nanosecond time scale and of some change in these motions due to ligand binding. However, several models for this motion (i.e., cone angle, time scale, and population) are accommodated by our data, and a unique description of the nanosecond motions is not possible. Moreover, the rates reflect the average of all five deuterons in the ring.

Since T_1 relaxation measurements using solution NMR are more common than those using solid-state NMR, it is worthwhile to contrast our interpretation of these T_1 values to that typical for solution samples. In the case of solid-state samples the nanosecond motions that drive relaxation processes are internal degrees of freedom (for example, local librations); there is no overall tumbling of the molecule contributing to relaxation, so deuterons without a librational or rapid hopping motion will not relax. As a consequence, subtle changes in the rate, angle, or populations produce a noticeable change in the T_1 times. For example, using a simple model for a two-site hopping motion, we estimated that a 15° libration angle near the Larmor frequency would change the relaxation times by orders of magnitude as compared, for example, with a 2° angle; in solution measurements, in the presence of an overall tumbling motion, such a 15° libration might produce as much as a 10% or a 50% effect on the relaxation rate, depending upon choice of overall

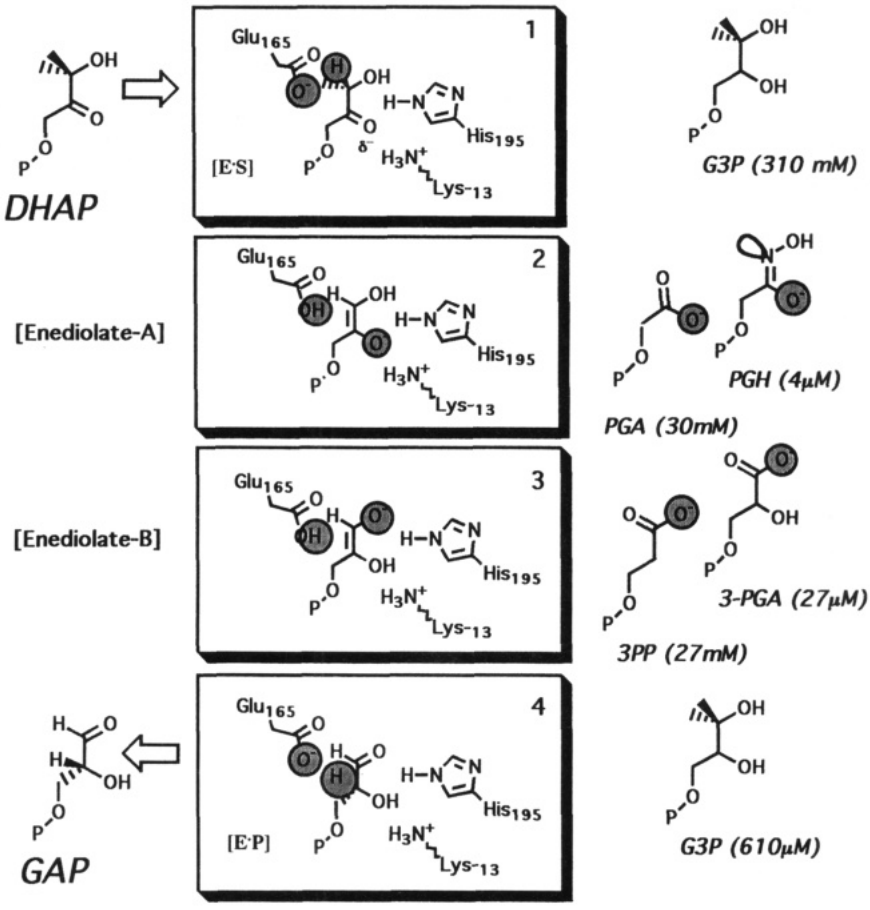

FIGURE 2: Catalytic pathway of TIM. The boxed figures indicate the proposed interactions of key protein residues with the substrate as GAP proceeds to DHAP along the catalytic pathway approximately based on previously proposed mechanisms (Albery & Knowles, 1976; Karplus et al., 1992). The species adjacent to the boxes are substrate and transition-state analogs that mimic the particular state. PGA and G3P were used as analog inhibitors in this study.

tumbling time, observation nucleus, etc. However, when nanosecond motions are studied by relaxation methods, spectral densities are not uniquely related to the correlation time. Aside from the fact that the angle might be unknown, a more fundamental problem results from the fact that relaxation is not a monotonic function of correlation time and goes through a minimum (the "T_1 minimum") in the nanosecond range: the correlation time is not a single-valued function of the relaxation rate. Therefore, the decrease in relaxation rate upon binding of G3P could be caused by either an increase or a decrease in correlation time. For this reason we will not discuss the differences between the samples.

T_1 values which are relatively short and yet exhibit little anisotropy, such as those observed for the ring-deuterated tryptophan in the loop, could be caused by any of a variety of different types of motion. For rigid parts of proteins one often proposes a small angle libration, and such a mechanism is certainly consistent with our data. For example, a libration has been observed previously in the deuterium NMR spectra of bacteriorhodopsin, which also gave rise to a short T_1 (Kinsey et al., 1981). A probable structural assignment for this libration would be oscillations in the dihedral angles χ_1 or χ_2; in that model the motions would pertain to the side chain only. The T_1 spectra could also be simulated by employing a two-site model with equal population at each site, an angle between the conformers of approximately 5−7°, and a rate of 10^8−10^9 s^{-1}.

An alternative to a typical librational motion would be a large angular excursion (such as an ~30−50° hopping motion) on the nanosecond time scale, which would also explain the efficient T_1 process. Such a model could be consistent with the observed line shape *only* if the populations for the two sites are very different (>10:1) because a nanosecond time-scale motion characterized by a large angular excursion and near equal populations would have a dramatic narrowing effect on the line shape and would give rise to T_1 anisotropy. Such a large-angle motion would be associated with backbone motions as well, since there is presumably a significant barrier to flipping the side chain without moving the backbone of the protein. Therefore, if large-angle fluctuations are responsible for the relaxation of deuterons in the ring, they would be expected to relax the α-deuteron as well.

We have also prepared a sample of TIM in which the tryptophan is deuterated at the α-position and which shows specific activity similar to that of the ring-deuterated sample. Using quantities comparable to those used for the ring-deuterated samples (50 mg), we failed to observe any signal in the α-labeled protein, even for very long acquisitions (>5000) with relaxation delays of approximately 10 s (or >50 000 transients with a delay of 1 s) , while the ring-labeled sample is easily observed within 100 transients and a delay of 1 s. A probable explanation for this failure is a long T_1 value for the backbone-labeled sample owing to a lack of motion on the nanosecond time scale. If the motions driving the relaxation of the ring deuterons are primarily side-chain dihedral fluctuations, then the backbone would not necessarily have these same librations. We conclude that it

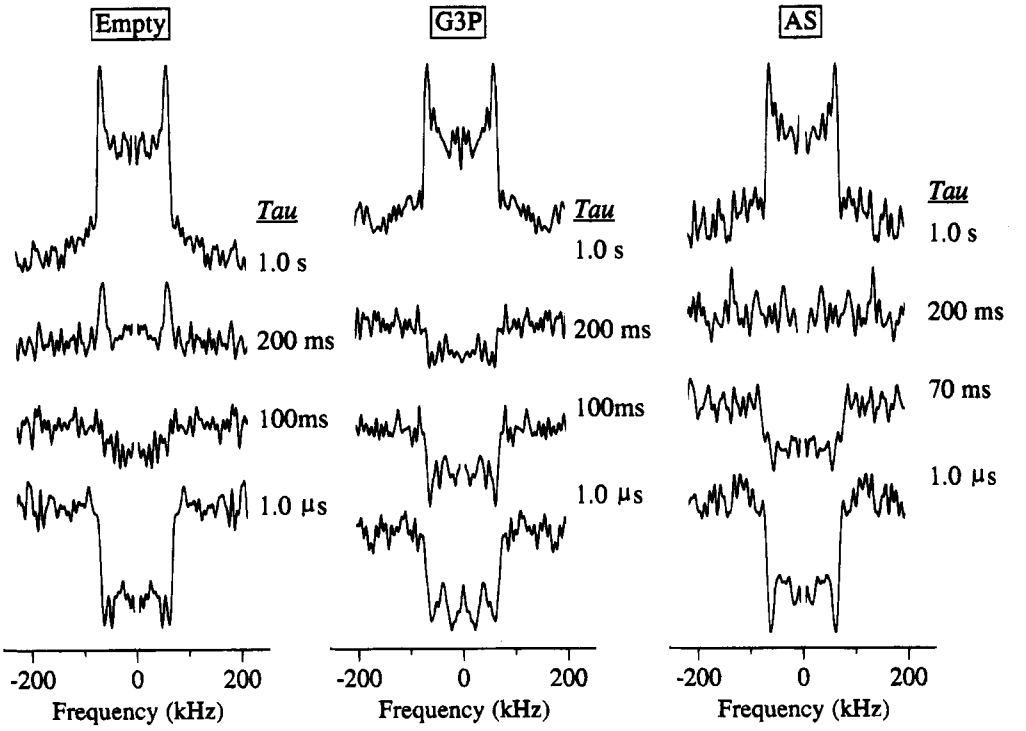

FIGURE 3: Deuterium SSNMR relaxation data of the ring-deuterated TIM mutant W90Y W157F with a single tryptophan at position W168. T_1 anisotropy spectra were collected using a nonselective inversion pulse followed by a variable delay and were detected using the quadrupole echo pulse sequence. The values calculated for T_1 for each series are within an order of magnitude of each other and probably reflect a small libration (<10°) near the Larmor frequency (60 MHz). T_1 values were 0.23 ± 0.05, 0.6 ± 0.2, and 0.28 ± 0.05 s for the empty TIM in PEG, the sample ligated with G3P, and the sample precipitated in ammonium sulfate, respectively. The short T_1 values for all samples allowed for short recycle times and hence better signal-to-noise ratios. These line shapes resemble static Pake powder patterns and are discussed further in the text.

is unlikely that the backbone of the loop moves substantially (>10°) on the nanosecond time scale. The lack of this signal, therefore, supports a model in which the relaxation mechanisms on the nanosecond time scale are local to the side chain, and presumably the loop opening and closing occurs on a slower time scale.

Dynamics on the Catalytic Time Scale and τ-Dependent Spectra. Motions with a characteristic frequency of the order of the quadrupole coupling constant have a pronounced effect on the line shape of the spectra. Since the quadrupole coupling constant is of the order ~200 kHz, motions with a characteristic frequency of 10^5-10^8 s^{-1} are spectroscopically observable. The introduction of an evolution period (τ) in between the initial pulse and the refocusing pulse allows us to probe motions occurring with time constants as long as approximately 5×10^3 s^{-1}. These rates are comparable to the catalytic time scale (k_{cat} = 4000−10 000 s^{-1}), and so τ-dependent quadrupolar echo spectra are of particular interest for this study.

The line shapes of the empty sample, the G3P-ligated sample, the PGA-ligated sample, and the ammonium sulfate precipitated sample, collected at a τ value of 30 μs, were all static-like spectra with quadrupolar coupling constants of 187 kHz (see Figure 4). These spectra are inconsistent with large-scale motion occurring at a rate faster than 10^5 s^{-1}, unless the motions are between two states of extremely unequal population (1:100). Additional spectra shown in Figure 4 were collected at τ values of 80 and 120 μs. In these spectra motions on the 10^4 s^{-1} time scale would cause decrease in intensity. Note in each case the ratio of intensity at the "horns" (±63 kHz) and the center of the spectrum, −20 to 20 kHz. Spectra of the empty enzyme, the G3P-ligated enzyme, and the ammonium sulfate precipitated enzyme show a decrease in the center of the spectrum as τ is increased. The horns do not decrease substantially as τ is increased. These line-shape effects were reproduced three times, and the differences between the 30-, 80-, and 120-μs spectra for each sample are far outside of the RMS deviations.

A deuteriotryptophan-labeled sample was prepared of wild-type TIM from *Typanosoma brucei*, which has five tryptophans including the one characterized in this work and four others that are not believed to move during catalysis. Preliminary τ-dependent quadrupolar echo spectra of this sample did not exhibit the loss in intensity for 120-μs refocusing delay as compared with 30 μs; the distortions in the line shape at long τ displayed in Figure 4 seem to be specific to the tryptophan in the flexible loop (unpublished work).

Simulations of the τ-dependent spectra were performed assuming a two-site model with three adjustable parameters: angular excursion, populations, and the rate between the sites. These parameters were independently varied in a systematic fashion. For simulations where the rate is less than 3×10^3 s^{-1}, or the angle of excursion is less than 20°, or the population between the two conformers differs by more than 2 orders of magnitude, we observed no change in the simulated spectra with echo delays of 30 and 120 μs. Spectra obtained for simulations with a rate greater than 10^6 s^{-1} and near equal populations did not reproduce the static-like spectra as observed for the data collected with a echo delay of 30 μs. Only simulations employing rates in the mid-kilohertz regime, angles between 20° and 60°, and population ratios between 1:1 and 20:1 produced static-like

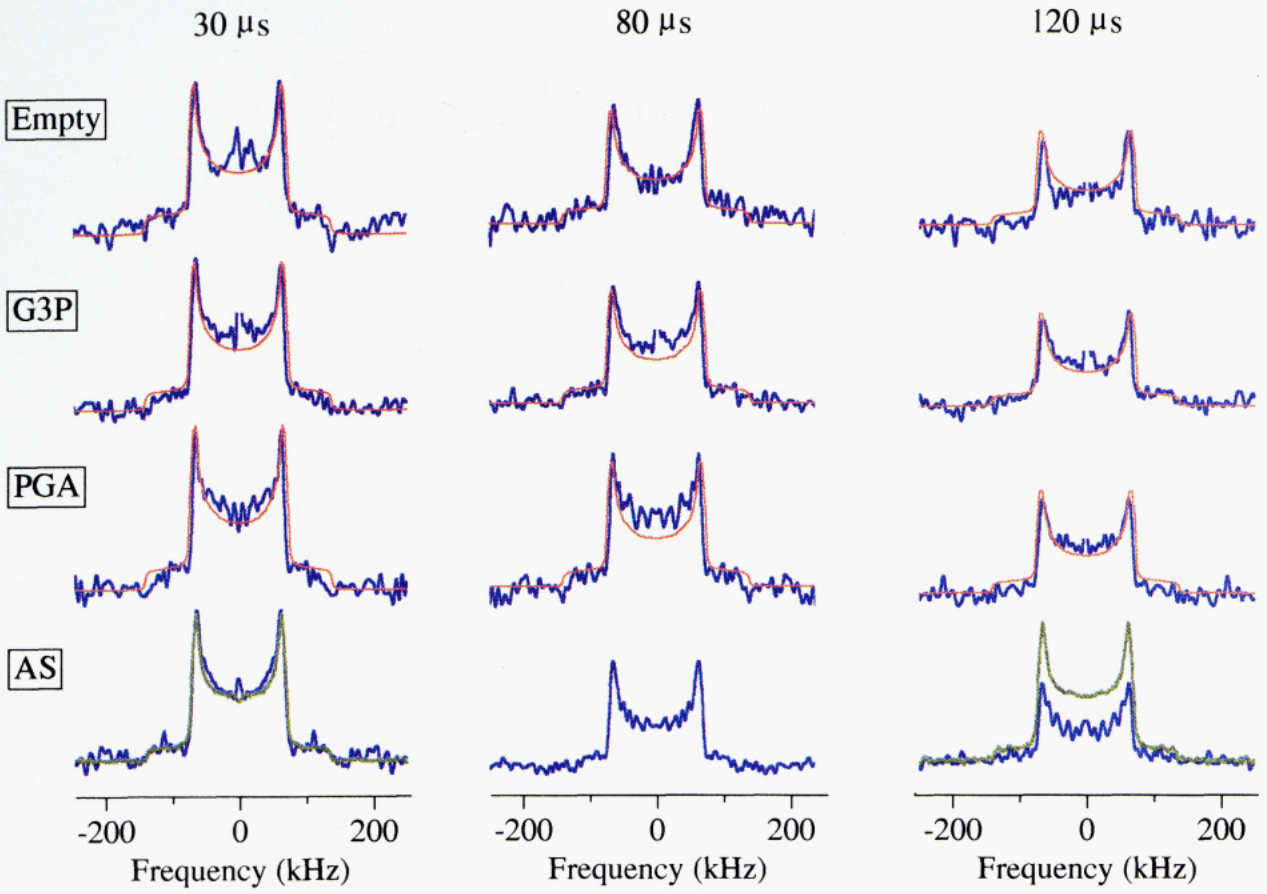

FIGURE 4: Deuterium SSNMR line-shape data of the ring-deuterated TIM mutant W90Y W157F with a single tryptophan at position W168. τ-dependent quadrupolar echo spectra are shown, representing approximately 30 000 scans for each spectrum. The pulse spacing is indicated at the top of each column. The blue and green traces correspond to the experimental data, and the red traces correspond to simulated spectra. In the order from top to bottom: ring-labeled TIM without substrate or transition-state analogs; ring-labeled TIM with G3P; ring-labeled TIM with PGA; ring-labeled TIM precipitated using ammonium sulfate. Data from ring-labeled tryptophan crystals (pure amino acid) are overlaid (green spectra) on the bottom right spectrum. The empty enzyme and the enzyme complexed with G3P and sulfate show a significant loss of spectral intensity, and the PGA-complexed TIM shows somewhat less intensity loss. This loss is particularly noticeable at frequencies about the center of the spectrum. Note that on the same time scale the crystallized (pure) ring-deuterated tryptophan shows no detectable loss of intensity because it is static in the crystal packing environment. The simulated spectra (red traces) correspond to a model employing a two-site jump with skewed populations. The angular excursion was determined from the crystal structures of the open and closed states. The populations were determined using the hole-burning sequence (see text). The best fits were judged from a series of simulations in which the population ratio and the rate were varied. The fits shown utilized a population ratio of 1:10 and a rate of transition from the more to the less populated form of 3×10^4 s^{-1} for the empty sample and the ammonium sulfate precipitated sample and 2×10^4 s^{-1} for the G3P- and PGA-ligated samples.

spectra at short echo delay times and decrease in intensity at longer echo delay times. It is these models that reproduce our data. The details of the decay in the signal with increasing delay can give some indications as to the population ratio, angle, and rate although multiple models will be consistent with a given spectrum. Nonetheless, the presence of mid-kilohertz motions with substantial angles is unmistakable so long as the populations are not different by a factor of 50 or more.

In the specific simulations shown (Figure 4), the angles used for the ring deuterons were obtained from the comparison of crystal structures: 18°, 30°, 39°, 44°, and 44° for ϵ, η, ζ, $\delta 1$, and $\delta 2$, respectively. These fits utilized a population ratio of 1:10 and a rate of transition from the more to the less populated form of 3×10^4 for the empty-labeled sample and the ammonium sulfate precipitated sample and 2×10^4 s^{-1} for the G3P and PGA samples. These best fits are shown as red traces placed over the experimental data. For the fits described above we estimated the error in the rates from measuring the signal to noise of the experimental data and RMS deviation between the different spectra as well as the RMS deviation between the simulated spectra. A conservative number for the error is 30% in each rate and a range of 20−50° in angle and a population ratio between 1:8 and 1:20.

Spectra taken at 35 °C of the empty TIM with ring-deuterated tryptophan (data not shown) indicated a slightly more rapid disappearance of the center of the spectrum as a function of τ. Although the rate increase implies an activated process, we were unable to analyze these data quantitatively in terms of an activation barrier. Using the assumed model of Arrhenius kinetics with a purely activated process and a preexponential factor of $h/2\pi kT$ together with the rate at 10 °C of 3×10^{-4} s^{-1} we obtain $E_{act} \sim 12$ kcal/mol. This assumed model is usually correct for simple thermally activated motions in crystalline solids near room temperature. It is well-known that motions in polymers often cannot be fit to such a model. Therefore, it is not obvious that this model applies well to a disordered portion of a protein.

In summary, the quadrupolar echo line-shape data are entirely consistent with a model in which the loop opens and closes on a time scale slightly faster than the enzyme turnover time, with unequal populations for the two states. The slow rate of the motion is assumed to be associated with

an inherent barrier in the protein. We did not prove this model; however, we can say that our data are inconsistent with a picture in which loop motions depend on ligand binding or in which the loop motion has a single or predominant correlation time in the nanosecond range.

Dynamics with Long-Time Scales and Hole-Burning Experiments. The DANTE inversion recovery experiment affords a separate and independent method for probing the dynamics of the C−D bond vector at relatively long times (Williams & McDermott, 1993). A selective pulse train burns a narrow hole in the deuterium powder pattern, thus selecting C−D bond vectors which have a particular polar angle to the applied field (here near 90°). Motion induced by loop movement would carry most of these bond vectors to a new polar angle giving rise to a new resonance condition and carry uninverted spectral density to "fill" the hole left in the powder pattern by the selective inversion. Following the recovery of the hole as a function of time gives independent information useful for simulating the τ-dependent spectra. In particular, the spectra in Figure 4 were compatible with a variety of combinations of populations and rates, and the hole-burning experiment can help us separate the rates and the populations. If the decrease in intensity resulted from motion involving two sites with nearly equal populations, then the hole would recover on the time scale of the motion and both population and rate would be independently measured. Such a result would be surprising in light of the crystallographic results. If the population ratio is more extreme than 1:10, then no recovery of the hole would be detectable.

The application of the selective pulse at ±63 kHz selected all C−D bond vectors that lay perpendicular to the applied field. These deuterons give rise to the largest intensity in the spectrum and hence give a higher signal to noise ratio. Spectra using the hole-burning pulse sequence were collected at recovery times of 100 ns, 1 μs, 10 μs, 100 μs, 1 ms, 10 ms, and 100 ms. A typical set of spectra using this pulse sequence is shown as the left column of Figure 5 with the reference spectrum superimposed on the 10-ms spectrum. The difference spectra shown in the right column were generated from DANTE spectra-minus-reference spectra scaled by the ratio of scans. Over this time course there is not an appreciable loss of intensity in the "hole", indicating that the motion evidenced in the quadrupolar echo experiment is associated with a skewed population. From the signal to noise ratio, we can place a lower limit on the population ratio: $P_1/P_2 > 8$. A plot of the normalized difference intensity as a function of time for each samples is shown in Figure 6. The effective upper limit in time that this method can probe is determined by the spin−lattice relaxation time, T_1. The dashed line in Figure 6 shows the expected loss of intensity due to the spin-lattice relaxation using the value of 250 ms as obtained for the T_1. We observe no decay in the intensity of inverted magnetization even after 10 ms or 100 times longer than the catalytic turnover rate.

As noted above, simulations of the τ-dependent spectra allow us to place an upper limit on the population ratio, $P_1/P_2 < 20$, if P_1 is assumed to be the population of the predominant conformer. The hole-burning experiment places a corresponding lower limit, $P_1/P_2 > 8$, which confirms the lower bound determined by the quadrupolar echo sequence. Although both the echo data and the DANTE hole-burning data indicate a substantial difference in the populations of

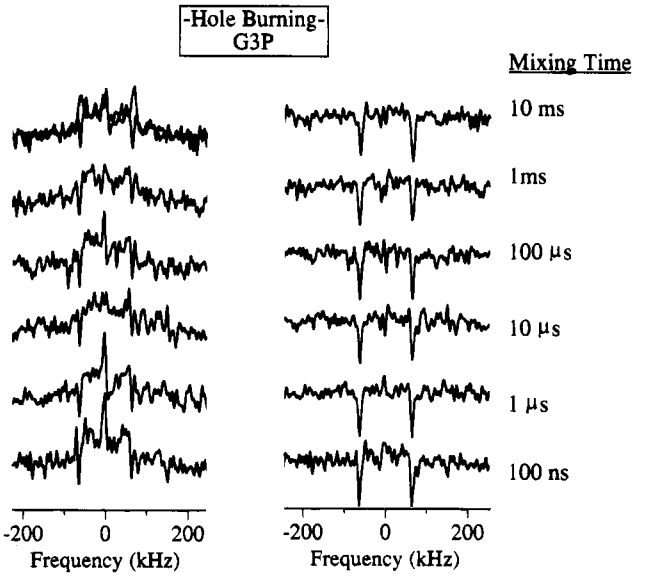

FIGURE 5: Deuterium SSNMR "hole-burning" data of the ring-deuterated TIM mutant W90Y W157F with a single tryptophan at position W168. The DANTE pulse sequence allowed us to selectively invert a narrow region of frequencies in the powder pattern and follow their evolution in time. Motion of the loop would carry the inverted region to a new frequency and cause the disappearance of the initial "hole". Detection after an evolution period much longer than the characteristic residence time of each conformer would directly report the population ratio of each conformer. The spectra shown here were obtained from the sample with G3P bound. The left column shows the holes at frequencies of ±63 kHz, corresponding to all deuterons laying along the *xy* plane. Note that there is no appreciable change in intensity of the hole even after 10 ms. This lack of change puts a limit on the ratio of the population of the two loop conformations such that $P_1:P_2 > 8:1$. Simulations of the τ-dependent quadrupolar echo spectra (Figure 4) using a more skewed population ratio place a lower limit of $P_1:P_2 < 20:1$, where P_1 is the population of the predominant conformer.

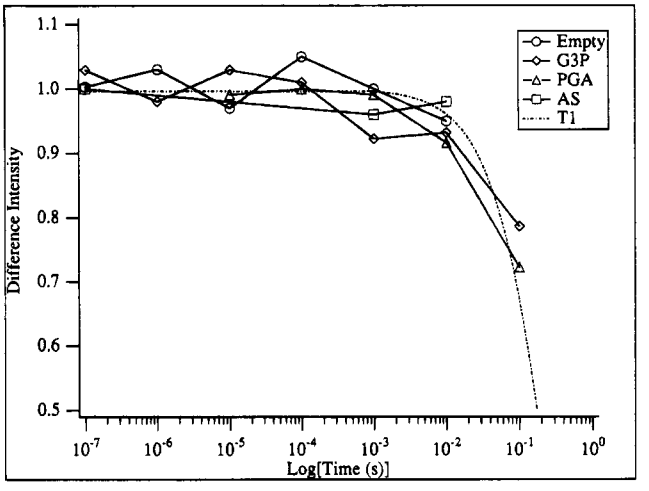

FIGURE 6: Intensities of the holes in the DANTE difference spectra (from deuterium SSNMR of the ring-deuterated TIM mutant with a single tryptophan at position W168) plotted as a function of time for all four samples: empty, ammonium sulfate, G3P, and PGA. The dotted line represents the spin−lattice relaxation behavior as measured with a nonselective pulse (Figure 3), given here because T_1 limits the overall time range for the hole-burning experiment.

the two structures of the loop for all samples, our data cannot distinguish which loop conformation is more populated. We assume that the X-ray crystallographic data report the structure of the dominant conformer in each case, since our

conditions for microprecipitation closely resemble those used for crystallization.

CONCLUSIONS

These spectra indicate two critical properties of the loop motion in TIM. First, the *rate for the most evident motion between the open and closed states is closely matched to the catalytic turnover rate.* Second, the τ-dependent spectra indicate that *loop motion on the time scale of enzyme turnover is not ligand gated* but is a natural motion of the protein. We find no evidence for ligand-gated motions on either the nanosecond or the catalytic time scale. The data do not support a nanosecond correlation time for the loop motion but indicate unambiguously that the loop does open and close on the 100-μs time scale, which very closely matches the catalytic rate.

These data disagree with a long-held assumption that the loop closure is ligand gated. They indicate also that product release would be allowed by a spontaneous opening of the loop which occurs in the presence of the ligand on a time scale slightly faster than turnover ($k_{open} = 3 \times 10^4$; $k_{cat} = 3 \times 10^3 - 10^4$ s^{-1}). TIM is a reversible enzyme, and the reactants and products are very similar. Consequently, a model in which substrate-like ligands close the loop would present a problem for product release. The natural rate of opening and closing on the near catalytic time scale would ensure that spontaneous opening of the loop while the intermediate is bound would be unlikely, yet product release would not be impeded either.

While this model is a substantial departure from the previous assumptions, it in no way disagrees with existing structural or kinetic data. The slow motion of the loop would imply a barrier to the motion, which would be of the order of 12 kcal/mol. It has been noted previously that the crystal structures of open and closed forms of TIM suggest the existence of a barrier of this order of magnitude associated with a Serine residue in an adjacent loop 7, which makes a large change in its dihedral angles (Wierenga et al., 1992). Mutants of TIM with altered loop motions are known and have been enzymatically characterized (Sampson & Knowles, 1992a,b); measurements of the dynamics of loops in these mutants would be of interest. It would also be of interest to examine other locations in the loop and other analog compounds.

The population ratio for the two states of the loop and the energetic barrier for opening and closing can be summarized in a cartoon, which explains a possible energy profile for loop motion (Figure 7). The barrier for motion is largely independent of ligand, but the relative energies of the two stable states of the loop do depend on the presence of the ligand. The cartoon is consistent with our data and others from the literature. The following features were summarized semiquantitatively. (1) The ligands have a pronounced effect on the relative populations of the two loop conformations as indicated by crystallography; the empty enzyme is mostly open, and the bound state is mostly closed. (2) The ligands are associated with a significant overall binding energy, as indicated by their inhibition dissociation constants. These dissociation constants were converted to binding energies and assigned as the energy difference for the open state in the empty enzyme and the closed state in the bound-state

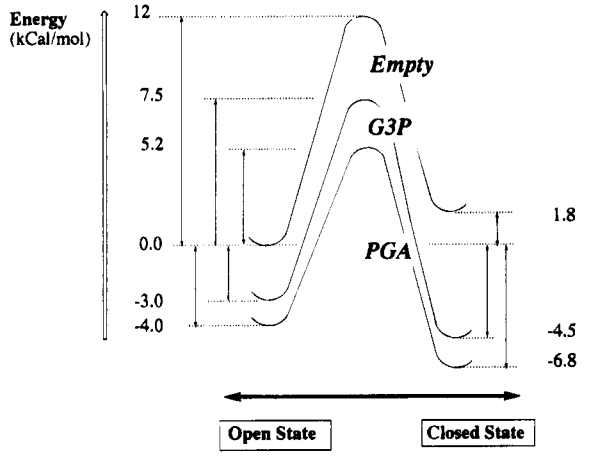

FIGURE 7: A cartoon version of an energy profile for loop closure that would be consistent with our data and several other considerations: crystallographic structures, inhibition dissociation constants, loop motion kinetics, and population ratios for the two conformations. A detailed description is given in the Conclusions section. The data indicate that in the open state of the loop ligands bind more weakly than in the closed state and that in the transition state of the motion the ligands bind with an intermediate affinity.

structure for the appropriate ligand. For example, for PGA the binding constant 10 μM gives an energy of -6.8 kcal/mol. (3) Our data indicate that the ligands have little effect on the kinetics of leaving the more populated site and that the barriers for opening a bound-state enzyme or for closing an open-state enzyme are of order 12 kcal/mol. (4) For all three samples the population ratio between open and closed states corresponds to an energy difference between 1.2 and 2.5 kcal/mol. (5) Combining these estimates, we come to the conclusion that the affinity of the open state for the ligands is significantly less than that of the closed state and the transition state for loop closing must have an intermediate affinity. (6) We note that the lower affinity of the open state is consistent with measurements of ligand binding constants in a "loopless" mutant (Pompliano et al., 1990) and nearly agrees quantitatively.

TIM is a special example of domain motion because the overall reaction is reversible and diffusion limited. It is of great interest to extend these measurements of conformational dynamics to enzymes with stronger driving forces and larger kinetic barriers.

ACKNOWLEDGMENT

We thank Dr. Rik Wierenga of the EMBL, Heidelberg, and Professor Greg Petsko, Brandeis University, for helpful discussions. We thank Professor Nicole Sampson of SUNY, Stonybrook, and Professor Jeremy Knowles of Harvard University for the plasmid coding for the mutant TIM used in these studies and Dr. David Goodin of Scripps Research Institute for the auxotrophic strain and for useful advice. The strain of *E. coli* used for tryptophan synthetase production was a generous gift of Professor Yanofsky of Stanford University. We thank Professor Bob Griffin of MIT for the programs used in simulating the deuterium spectra. We thank Alona Cohen and Marco Cavagna for their considerable assistance in the characterization of the kinetics of TIM microprecipitates.

REFERENCES

Alber, T., Banner, D. W., Bloomer, A. C., Petsko, G. A., Phillips, D., Rivers, P. S., & Wilson, I. A. (1981) *Philos. Trans. R. Soc. London B 293*, 159−171.

Albery, W. J., & Knowles, J. R (1976) *Biochemistry 15*, 5588−5600.

Beshah, K., Olejniczak, E. T., & Griffin, R. G. (1987) *J. Chem. Phys. 86*, 4730−4736.

Blacklow, S. C., Raines, R. T., Lim, W. A., Zamore, P. D., & Knowles, J. R. (1988) *Biochemistry 27*, 1158−1167.

Branden, C., & Tooze, J. (1991) in *Introduction to Protein Structure*, p 302, Garland Publishing, Inc., New York and London.

Brown, F. K., & Kollman, P. A. (1987) *J. Mol. Biol. 198*, 533−546.

Chothia, C., Lesk, A. M., Tramontano, A., Levitt, M., Smith-Gill, S. J., Air, G., Sheriff, S., Padlan, E. A., Davies, D., Tulip, W. R., Colman, P. M., Spinelli, S., Alzari, P. M., & Poljak, R. J. (1989) *Nature 342*, 877−883.

Chung, C. T., Niemela, S. L., & Miller, R. H. (1989) *Proc. Natl. Acad. Sci. U.S.A. 86*, 2172−2175.

Copié, V., McDermott, A. E., Beshah, K., Williams, J. C., Spijker-Assink, M., Gebhard, R., Lugtenburg, J., & Griffin, R. G. (1994)-*Biochemistry 33*, 3280−3286.

Davenport, R. C., Bash, P. A., Seaton, B. A., Karplus, M., Petsko, G. A., & Ringe, D. (1991) *Biochemistry 30*, 5821−5826.

Drewe, W. F., & Dunn, M. F. (1985) *Biochemistry 24*, 3977−3987.

Falzone, C. J., Wright, P. E., & Benkovic, S. (1994) *Biochemistry 33*, 439−442.

Griffin, R. G. (1981) in *Solid state NMR of Lipid Bilayers* (Lowenstein, J. M., Ed.) p 842, Academic Press, New York.

Hart, K. W., Halsall, D. J., & Holbrook, J. J. (1993) in *Genetically Inserted Tryptophans in Protein Spectroscopy* (Clark, R. J. H., & Hester, R. E., Ed.) pp 195−226, John Wiley and Sons, New York.

Hiyama, Y., Silverton, J. V., Torchia, D. A., Gerig, J. T., & Hammond, S. J. (1986) *J. Am. Chem. Soc. 108*, 2715−2723.

Joseph, D., Petsko, G. A., & Karplus, M. (1990) *Science 249*, 1425−1428.

Karplus, M., Evanseck, J. D., Joseph, D., Bash, P. A., & Field, J. (1992) *Faraday Discuss. 93*, 239−248.

Kempner, E. S. (1993) *FEBS Lett. 326*, 4−10.

Keniry, M. A., Gutowsky, H. S., & Oldfield, E. (1984) *Nature 307*, 383−386.

Kinsey, R. A., Kintanar, A., & Oldfield, E. (1981) *J. Biol. Chem. 256*, 9028−9036.

Knowles, J. R., & Albery, W. J. (1977) *Acc. Chem. Res. 10*, 105−110.

Leszczynski, J. F., & Rose, G. D. (1986) *Science 234*, 849−855.

Lipari, G., & Szabo, A. (1982) *J. Am. Chem. Soc. 104*, 4546−4559.

Lolis, E., & Petsko, G. A. (1990) *Biochemistry 29*, 6619−6625.

Lolis, E., Alber, T., Davenport, R. C., Rose, D., Hartman, F. C., & Petsko, G. A. (1990) *Biochemistry 29*, 6609−6618.

Matthews, H. R., Matthews, K. S., & Opella, S. J. (1977) *Biochim. Biophys. Acta 497*, 1−13.

Noble, M. E. M., Wierenga, R. K., Lambeir, A-M., Opperdoes, F. R., Thunnissen, A-M. W. H., Kalk, K. H., Groendijk, H., & Hol, W. G. J. (1991) *Proteins: Struct., Funct., Genet. 10*, 50−69.

Peng, J. W., & Wagner, G. (1992) *J. Magn. Reson. 98*, 308−332.

Pompliano, D. L., Peyman, A., & Knowles, J. R. (1990) *Biochemistry 29*, 3186−3194.

Rice, D. M., Wittebort, R. J., Griffin, R. G., Meirovitch, E., Stimson, E. R., Meinwald, Y. C., Freed, J. H., & Scheraga, H. A. (1981) *J. Am. Chem. Soc. 103*, 7707−7710.

Rose, I. A. (1962) *Brookhaven Symp. Biol. 15*, 293−309.

Sampson, N. S., &. Knowles, J. R. (1992a) *Biochemistry 31*, 8482−8487.

Sampson, N. S., & Knowles, J. R. (1992b) *Biochemistry 31*, 8488−8494.

Schneider, W. P., Nichols, B. P., & Yanofsky, C. (1981) *Proc. Natl. Acad. Sci. U.S.A. 78*, 2169−2173.

Speyer, J. B., Weber, R. T., Das Gupta, S. K., & Griffin, R. G. (1989) *Biochemistry 28*, 9569.

Spiess, H. W. (1980) *J. Chem. Phys. 72*, 7655−7662.

Tomita, Y., O'Connor, E. O., & McDermott, A. E. (1994) *J. Am. Chem. Soc. 116*, 8766−8771.

Usha, M. G., Peticolas, W. L., & Wittebort, R. J. (1991) *Biochemistry 30*, 3955−3962.

van der Berg, E. M. M., van Liemt, W. B. S., Heemskerk, B., & Lugtenburg, J. (1989) *Recl. Trav. Chim. Pays-Bas 108*, 304−313.

Verlinde, C. L. M. J., Noble, M. E. M., Kalk, K. H., Groendijk, H., Wierenga, R. K., & Hol, W. G. J. (1991) *Eur. J. Biochem. 198*, 53−57.

Vold, R. R., & Vold, R. L. (1991) in *Deuterium Relaxation in Molecular Solids* (Warren, W., Ed.) pp 85−166, Academic Press, New York.

Wade, R. C., Davis, M. E., Luty, B. A., Madura, J. D., & McCammon, J. A. (1993) *Biophys. J. 64*, 9−15.

Waldman, A. D. B., Hart, K. W., Clarke, A. R., Wigley, D. B., Barstow, D. A., Atkinson, T., Chia, N. W., & Holbrook, J. J. (1988) *Biochem. Biophys. Res. Commun. 150*, 752−759.

Wierenga, R. K., Noble, M. E. M., Vriend, G., Nauche, S., & Hol, W. G. J. (1991a) *J. Mol. Biol. 220*, 995−1015.

Wierenga, R., Noble, M. E. M., Postma, J. P. M., Groendijk, H., Kalk, K. H., Hol, W. G. J., & Opperdoes, F. R. (1991b) *Proteins: Struct., Funct., Genet. 10*, 33−49.

Wierenga, R. K., Borchert, T. V., & Noble, M. E. M. (1992) *FEBS Lett. 307*, 34−39.

Williams, J. C., & McDermott, A. E. (1993) *J. Phys. Chem. 97*, 12393−12398.

Wittebort, R. J., Olejeniczak, E., & Griffin, R. G. (1987) *J. Chem. Phys. 86*, 5411.

BI941746A